DISRUPTION CRITERIA AND POST-IMPACT VOID FRACTIONS FOR BRICK-PILE PLANETESIMALS. D. G. Korycansky, E. Asphaug, *CODEP, Department of Earth and Planetary Sciences, University of California, Santa Cruz CA 95064* .

In this work we report on critical disruption criteria (Q^*_{RD}) and void fractions after collisions for so-called "brick-pile" planetesimals of ~ 1 km diameter. The calculations were carried out using a rigid-body dynamics simulation program written by use that employs the Open Dynamics Engine (ODE, `www.ode.org`), an open-source package that models rigid-body motion for multi-body simulation including collisions and friction. ODE contains sophisticated collision-detection and constraint-force solvers for compact many-body configurations [1].

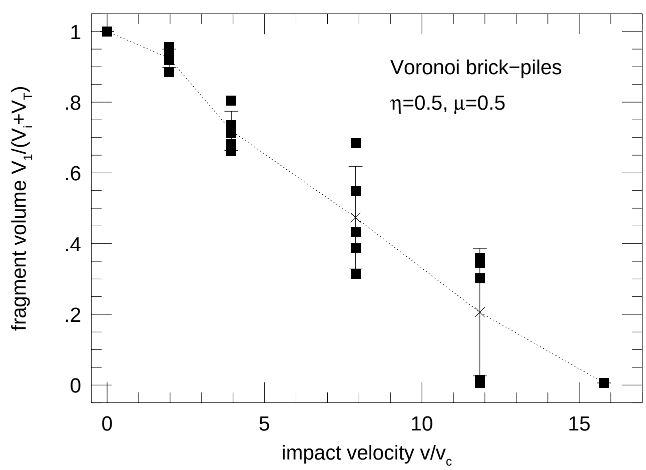

Figure 1: Volume ratio of largest fragments to total volume of impactor and target, vs impact velocity v_i scaled to critical velocity v_c, for a runs where the coefficient of friction $\mu = 0.5$ and restitution $\varepsilon = 0.5$.

Critical Disruption Criteria

Similar work carried out by us for rubble-pile bodies has been previously described by us [2]. The work reported here involves so-called "brick piles", i.e. bodies made of close-fitting macro-scale fragments with no initial void space or porosity. In particular, we study the effects on two different kinds of structures: 1) irregular structures based on Voronoi tessellation of points quasi-randomly distributed inside an irregular icosahedron that is a simple model of a small asteroid, and 2) cubical arrays of cubic elements. In both cases, the target objects are made of 1000 initial elements (a $10 \times 10 \times 10$ array in the cubical case). For comparison with results given by our previous work, the mass of the target objects is 8×10^{12} kg, and the mass ratio of the impactor to target is 1:1000. As before, we determine Q^*_{RD} by running a suite of impacts at different relative velocities v_i and interpolate for the impact velocity for which the mass of the largest fragment is one half the total mass $m_i + m_T$, and calculate the corresponding kinetic energy per unit mass. We use the so-called reduced critical disruption value introduced by [4,5] (though for this mass ratio, there is little difference between Q^*_{RD} and the original criterion denoted by Q^*_D). Additionally, given the stochasticity of the impact and disruption processes, five runs with differing (random) target orientations were done at each velocity.

Parameters of interest also include the friction coefficient μ and coefficient of restitution ε. Three combinations were run in our previous work: low ($\mu = 0, \varepsilon = 0.8$), medium ($\mu = 0, \varepsilon = 0.5$), and high-dissipation cases ($\mu = 0.5, \varepsilon = 0.5$). We have run calculations with the same combination of parameters here. An example of volume (or mass) ratio of largest fragments vs. velocity is shown in Fig. 1, where velocities are scaled to the the critical velocity $v_c = M(6G/5\mu R)^{1/2}$. Here $M = m_i + m_T$ is the sum of the masses of two colliding bodies (rubble piles) m_i and m_T, equivalent spherical radii $R = (R_i^3 + R_T^3)^{1/3}$, and the reduced mass $\mu = m_i m_T/(m_i + m_T)$. For the cases shown here, $v_c = 2.53 \times 10^1$ m s^{-1} [3].

Results of the analysis for the comparison are shown in Table I. The left two columns give Q^*_{RD} in Joules kg^{-1} for rubble piles from our previous work [4]; the different results are for loose-fitting rubble piles made of elements with an internal mass disribution of a single mass (a "monodisperse" distribution), and a power-law distribution which the number of elements of mass m or greater $n(> m) \propto m^{-1}$. The right two columns give the new results for brick-pile targets. The main result of Table I is that (surprisingly) brick-pile objects are easier to disrupt than rubble-pile ones. Low-dissipation collisions for cubic arrays are highly uncertain, and may not represent stable post-impact piles. The difference between the previous and present results is largest for the high-dissipation cases. It may be the case that loosely-integrated rubble piles absorb and dissipate the kinetic energy of the impact more strongly than brick-piles, despite expectations of greater surface contact between elements (and higher friction) for the latter type of objects.

Post-collision Porosity

The second phase of the work reported here are measured void fractions, or porosities, of post-collision rubble piles. Again, the initial bodies are brick-piles with either Voronoi decomposition construction or cubic arrays. We measured the internal void space by means of computing the volumes of a

		Rubble pile		Brick pile	
μ	ε	monodisperse	power-law	Voronoi	cubic
0.0	0.8	3.3 ± 1.2	9.7 ± 3.1	2.2 ± 1.8	(0.05 ± 0.05)
0.0	0.5	20.7 ± 5.7	31.1 ± 13.2	12.2 ± 4.8	14.8 ± 9.8
0.5	0.5	67.6 ± 9.2	93.9 ± 25.2	17.9 ± 1.0	15.8 ± 6.5

Table 1: Reduced critical disruption criteria Q^*_{RD} for km-scale rubble piles (target mass $m_T = 8 \times 10^{12}$ kg). Values of Q^*_{RD} are given in units of J kg^{-1}.

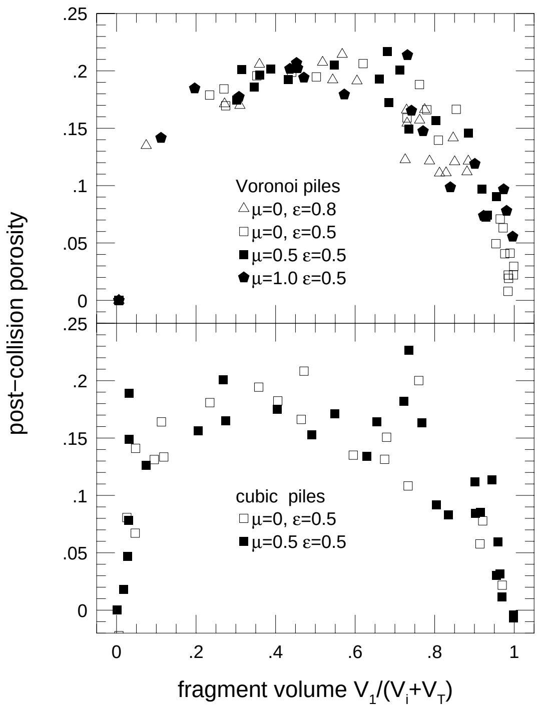

Figure 2: Porosity fraction vs. relative volume of the largest fragment for impacts into Voronoi brick-piles (top panel) and cubic brick-piles (bottom).

10,240-faced polyhedron that was "shrink-wrapped" around the largest fragment at the end of the calculation. The volume of the shrink-wrapped polyhedron was compared to the summed volumes of the constituents of the fragment to derive a void fraction, i.e. the (macro-) porosity of the final object.

Results are displayed in Fig. 2, where the porosity of post-impact objects is plotted as a function of volume V_1 of the largest fragment relative to the total volume $V_i + V_T$ of the impactor + target. We are concerned primarily with static configurations, that is, the post-impact structures; plotting porosity as a function of fragment volume V_1 is primarily a means of separating the results into a more graphically obvious form. The overall trend of porosity vs. V_1 is partly a function of impact disruption: Low-velocity impacts induce small amounts of volume loss and minimal rearrangements, so that porosity drops to zero as $V_1 \rightarrow V_i + V_T$. On the other hand, higher-velocity impacts are more disruptive ($V_1 \rightarrow 0$), laving behind fewer elements and less opportunity for internal voids.

The top panel shows calculations involving Voronoi targets, while the lower panel shows results for cubic-array targets. For both kinds of target objects, calculations were performed for different values of friction and restitution coefficients to see if porosity would be a function of frictional coefficients. We added an additional set of calculations for $\mu = 1$, $\varepsilon = 0.5$.

In general, we find it difficult or impossible to generate porosity values much larger than $\sim 20\%$. In this scenario, macro-porosity is generated by the mis-aligned rearrangement after an impact of initially close-fitting blocks. It is well known that the densities of many asteroids are significantly lower than expected from the values for monolithic rock; porosity values of up to $\sim 50-60\%$ have been inferred [6]. This is strong evidence of rubble-pile or aggregate composition. It is unknown whether the inferred porosity is "micro" or "macro" in structure, that is, whether the under-density is produced by small cavities in the mineral structure, or by large voids among loosely stacked blocks. Our scenario cannot at the moment account for the larger values of porosity observed, but it may play a role. At the same time, we hesitate to make a definitive statement, as our efforts do not as yet include a model for strong cohesive forces (e.g. static friction or its equivalent surface effects) that may play a role in holding large-scale structures in place.

Acknowledgments

This work is supported by the NASA's Planetary Geology and Geophysics Program, under award NNX07AQ04G.

References

[1] Erleben *et al.* (2005) *Physics-Based Animation*, Charles River Media, Inc. [2] Korycansky and Asphaug 2009, *Icarus* **204**, 316. [3] Leinhardt *et al.* 2000, *Icarus* **146**, 133. [4] Leinhardt and Stewart 2009, *Icarus* **199**, 542. [5] Stewart and Leinhardt 2009, *Ap. J. Lett.* **691**, L133. [6] Britt and Consolmagno 2001, *Icarus* **152**, 134.